ResearchGate

See discussions, stats, and author profiles for this publication at: https://www.researchgate.net/publication/327106848

Application of metallurgical slag to treat geothermal wastewater with high concentrations of arsenic and boron

Article *in* International journal of Environmental Science and Technology · August 2018

DOI: 10.1007/s13762-018-1952-z

CITATIONS
0

READS
137

4 authors:

B. M. Mercado-Borrayo
Universidad Nacional Autónoma de México
8 PUBLICATIONS **40** CITATIONS

SEE PROFILE

Myriam Solís
Center for Research and Advanced Studies of the National Polytechnic Institute
14 PUBLICATIONS **29** CITATIONS

SEE PROFILE

Rafael Schouwenaars
Universidad Nacional Autónoma de México
98 PUBLICATIONS **457** CITATIONS

SEE PROFILE

Rosa Maria Ramírez Zamora
Universidad Nacional Autónoma de México
81 PUBLICATIONS **396** CITATIONS

SEE PROFILE

Some of the authors of this publication are also working on these related projects:

Project

Implementation of thermosolar, photovoltaic and photocatalytic energy for the removal of heavy metals: design of a self-sustainable pilot plant View project

Project

Write a review View project

All content following this page was uploaded by Rosa Maria Ramírez Zamora on 24 April 2019.

The user has requested enhancement of the downloaded file.

International Journal of Environmental Science and Technology
https://doi.org/10.1007/s13762-018-1952-z

ORIGINAL PAPER

Application of metallurgical slag to treat geothermal wastewater with high concentrations of arsenic and boron

B. M. Mercado-Borrayo[1] · M. Solís-López[2] · R. Schouwenaars[2] · R. M. Ramírez-Zamora[1]

Received: 5 June 2017 / Revised: 17 June 2018 / Accepted: 3 August 2018
© Islamic Azad University (IAU) 2018

Abstract

The reuse of geothermal wastewater for irrigation is an attractive alternative for supplying water demand in agriculture, due to the high volumes generated in geothermal plants. This application is limited by the presence of toxic semimetals such as arsenic and boron, which generally require high-cost commercial adsorbents for removal. This work studies the removal mechanism and process optimization of arsenic and boron, present in high concentrations in synthetic solutions and in geothermal wastewater, using metallurgical slags. The effect of pH, initial concentration of arsenic and boron and slag dose were investigated using a 3^3 factorial experimental design and response surface method to optimize the operating conditions of the removal of pollutants. Scanning electron microscope analysis showed that the removal mechanism consisted in a dissolution–precipitation reaction rather than adsorption. The effluent produced from wastewater at the optimal operating conditions in a two-step process meets the criteria proposed for both metalloids by the US Environmental Protection Agency for water used for irrigation.

Keywords Agricultural irrigation · Chemical precipitation · Metals removal · Wastewater reuse

Introduction

Arsenic (As) and boron (B) are metalloids representing environmental and health risks, even though boron is also an essential micronutrient for plants. However, excess levels of B in irrigation water have harmful effects for several crops (Liu et al. 2014). Arsenic can produce chronic diseases in humans and affects crops as well. For drinking water, the guidelines recommended by the World Health Organization establish concentration limits of 0.01 mg/L As and 2.4 mg/L B (WHO 2011).

For irrigation water, the effect of As and B is distinct. Although As affects the physiology of plants (Garg and Singla 2011; Smith et al. 2010), the primary concern is human health. Limits for As in irrigation are related to the risks of accumulation of this element in plants and its introduction in the food chain, either through direct consumption of contaminated plants or through animal fodder. The US EPA guideline is fixed at 0.1 mg/L (US EPA 2012). This value is independent of the crop under consideration. Even though US EPA mentions that As toxicity to plants varies widely, ranging from 0.5 mg/L for bush beans to 5 mg/L for kale (US EPA 2012).

Boron, on the other hand, is essentially less toxic for humans and plant tolerance determines its maximum allowable levels in irrigation water, where tolerance is defined as the ability of a crop to maintain yield in the presence of disease (which may in turn be caused by contaminants) (Newton 2016). Table 1 shows the relationship between boron levels and the tolerance of various crops (Ayers and Westcot 1994; Moss and Nagpal 2003).

Given the acute shortage of conventional water resources, the use of non-convectional resources is currently investigated. At present, municipal wastewater and rainwater are alternative water supplies for irrigation (Petousi et al. 2015). Another source for irrigation can be wastewater generated in geothermal power plants, due to the high volumes produced

Editorial responsibilty: Tanmoy Karak.

✉ R. M. Ramírez-Zamora
RRamirezZ@iingen.unam.mx

[1] Instituto de Ingeniería, Coordinación de Ingeniería Ambiental, Universidad Nacional Autónoma de México, Cd. Universitaria, Coyoacán, 04510 Ciudad de México, México

[2] Departamento de Materiales Y Manufactura DIMEI, Facultad de Ingeniería, Universidad Nacional Autónoma de México, Avenida Universidad 3000, Coyoacán, 04510 Ciudad de México, México

Published online: 19 August 2018

Table 1 Sensitivity of Different Crops to Boron (Moss and Nagpal 2003; Ayers and Westcot 1994). Tolerance is defined as the limit of B at which the crop is still economically viable (Newton 2016)

Very sensitive	Sensitive	Moderately sensitive	Moderately tolerant	Tolerant	Very tolerant
< 0.5 mg/L B	0.5–1 mg/L B	1–2 mg/L B	2–4 mg/L B	4–6 mg/L B	6–15 mg/L B
Citrus limon (Lemon)	*Persea americana* (Avocado)	*Capsicum annuum* (Pepper)	*Lactuca sativa* (Lettuce)	*Sorghum bicolor* (Sorghum)	*Gossypium hirsutum* (Cotton)
Rubus spp. (Blackberry)	*Citrus X paradisi* (Grapefruit)	*Pisum sativa* (Pea)	*Brassica oleracea* (Cabbage)	*Lycopersicon lycopersicum* (Tomato)	*Asparagus officinalis* (Asparagus)
	Citrus sinensis (Orange)	*Daucus carota* (Carrot)	*Apium graveolens* (Celery)	*Medicago sativa* (Alfalfa)	
	Prunus armeniaca (Apricot)	*Raphanus sativus* (Radish)	*Brassica rapa* (Turnip)	*Petroselinum crispum* (Parsley)	
	Prunus persica (Peach)	*Solanum tuberosum* (Potato)	*Avena sativa* (Oats)	*Beta vulgaris* (Beet red)	
	Prunus avium (Cherry)	*Cucumis sativus* (Cucumber)	*Zea mays* (Maize)		
	Prunus domestica (Plum)		*Cynara scolymus* (Artichoke)		
	Diospyros kaki (Persimmon)		*Nicotiana tabacum* (Tobacco)		
	Vitis vinifera (Grape)		*Brassica juncea* (Mustard)		
	Juglans regia (Walnut)				
	Allium cepa (Onion)				
	Allium sativum (Garlic)				
	Ipomoea batatas (Sweet potato)				
	Triticum eastivum (Wheat)				

in these facilities (average value of 9.5 m^3/h * MW). However, this source has high concentrations of toxic metalloids, such as boron and arsenic (Finster et al. 2015).

Mexico is the fourth largest geothermal electricity producer worldwide, exploiting four fields through the Federal Electricity Commission Comisión Federal de Electricidad (CFE): Cerro Prieto (720 MWe), Los Azufres (88 MWe), Los Humeros (35 MWe) and Las Tres Vírgenes (10 MWe). Direct applications of geothermal wastewater have been evaluated at the Mexican geothermal field Los Azufres, including a wood-dryer, a greenhouse and a heating system for the CFE facilities (Hiriart and Gutiérrez-Negrín 2003). However, the direct reuse of geothermal wastewater for irrigation has not yet been assessed due to the high concentration of metalloids (approximately 6 mg/L As and 600 mg/L B). Therefore, it is important to develop a cost-effective treatment for these pollutants, capable of dealing with these high concentrations.

One of the most used technologies for the removal of arsenic and boron from wastewater is reverse osmosis (RO). The rejection of boron by RO is limited, and approximately 40–78% of the influent boron content is normally found in the permeate (Samatya et al. 2015). Membrane processes removing B from geothermal and seawaters were studied by Tomaszewska and Bodezek (2013), Wang et al. (2014) and Güler et al. (2015), who focused their investigations on the evaluation of operating factors to improve the removal of this metalloid by RO. Nevertheless, this process has shown low removal efficiencies of boron when the initial concentration of this pollutant is high (Table 2).

Coupling ion exchange with commercial boron selective resins and ultrafiltration is another approach investigated for boron removal. The main advantage of this method is its high efficiency and relatively low cost, using only ion exchange, and the drawbacks of this process are the regeneration of exhausted resins and the conditioning stage (with

Table 2 Removal efficiencies of boron at different initial concentrations by RO

Initial concentration (mg/L B)	% Removal	References
2.5	56	Tomaszewska and Bodzek (2013)
5	55–93	Wang et al. (2014)
5	83–93	Güler et al. (2015)
8.98	48	Tomaszewska and Bodzek (2013)
96.73	12	Tomaszewska and Bodzek (2013)

pH varying from 2 to 11 depending on the specific treatment), which increase the treatment costs (Kabay et al. 2013). This cost can also increase from 0.2 to 3.2 cent€/m^3 when membranes and resins are used simultaneously (Chillón et al. 2011).

Adsorption has also been used for the removal of these metalloids from water. However, this process can be very expensive due to the cost of the commercial adsorbents (Mohan and Pittman 2007; Ungureanu et al. 2015), especially because of the high doses required for removing pollutants at elevated initial concentrations. In addition, this process has not yet been evaluated for treating geothermal wastewater. Therefore, the use of low-cost adsorbents is an alternative for the removal of contaminants present in high concentration (Wu et al. 2014; Kalel et al. 2017).

Metallurgical slags of the steel and iron-making industries are an interesting option to be used as low-cost adsorbents, due to their high availability and chemical composition (Wu et al. 2014). An earlier study by the authors showed that the removal of As(V) and B using slag shows a significant economic advantage with respect a commercial product, because the estimated total treatment cost using slag was almost 60% lower (0.4 vs. 0.96 €/m^3) (Mercado-Borrayo et al. 2014). The production of more than 400 million tons each year of iron and steel slag (Worldsteel Association 2014) can easily fulfill the market demand for water treatment while reducing environmental problems associated to its disposal, since most slags are still disposed in landfills. At the moment of writing, the most common use of slag is as a partial substitute of Portland cement in concretes (Kourounis et al. 2007). A broad review on the use of metallurgical slag in environmental applications was provided recently by Mercado-Borrayo et al. (2018a, b).

Research on the use of slag for water treatment over the last decade has focused on the properties of its constituents (oxides of Fe, Si, Mg, Al and Ca) as related to the removal metals (Mercado-Borrayo et al. 2018a, b), phosphate (Oguz 2005), dyes (Gupta and Suhas 2009) and organic compounds (Lee et al. 2009). Proposed removal mechanisms were based on adsorption/co-precipitation, redox reaction and electrostatic interaction. In the specific case of As and B, adsorption has been proposed as the governing mechanism (Piatak et al. 2015).

The experimental part of this research was performed at the laboratories of the Environmental Engineering Department of the Engineering Institute, UNAM in 2013; additional characterization of the slag and data analysis were performed in the period of 2015–2017, at the same department and the department of Materials and Manufacturing of the Faculty of Engineering, UNAM. The goal was to optimize the removal of arsenic(V) and boron by means of metallurgical slags, present in high concentrations in synthetic solution and geothermal wastewater, with the goal of producing an effluent for irrigation reuse. The question on the nature of the removal mechanism will also be addressed.

Materials and methods

Materials

Experiments were carried out using steel slag (Slag-1) and iron slag (Slag-2). These materials were characterized in a previous work (Mercado-Borrayo, 2013). X-ray diffraction (XRD) was done on a Bruker D8 Advance diffractometer in a 2θ range from 10° to 70°. The identification of crystalline phases was performed using the Powder Diffraction File; quantification was done using the Rietveld method with the Fullprof 2000 program. The surface characteristics were determined by the nitrogen physical adsorption technique using a Belsorp Mini II. The zeta potential (pH_{pzc}) was measured at 150 V with 60 Hz cycles with Zeta-Meter using slag suspensions of 0.1 g/L in distilled water over the pH range of 3–9. Further details can be found in Mercado-Borrayo et al. (2013); results are summarized in Table 3. The arsenic and boron reagents utilized to prepare solutions were $Na_2HAsO_4{\cdot}7H_2O$, 98.1%, Sigma-Aldrich and boric acid, Bruker, 99.9%.

Systems and experimental techniques

Removal tests of arsenic and boron from synthetic solutions

A response surface strategy was followed on a 3^3 experimental grid by fitting a second-degree polynomial to the 27 data points obtained for each slag and pollutant (108 experiments). Contrary to a 3^3 factorial design, where replicates

Table 3 Principal characteristics of the slags used

	Slag 1	Slag 2
XRD	38% by weight of $Mg(OH)_2$ 30% by weight of $Ca(OH)_2$ 13% by weight of $CaFe_2O_4$	55% by weight of iron oxides, present in form αFeO(OH), γ-Fe_2O_3 and/or Fe_3O_4 31% by weight of $Mg(OH)_2$
SBET	Specific surface area: 7.34 m^2/g Pore volume: 2.78 E−02 cm^3/g Pore diameter: 15.09 nm	Specific surface area: 0.3 4 m^2/g Pore volume: 3.61 E−03 cm^3/g Pore diameter: 42.74 nm
pHpzc	8.5	6.5

of each point are needed to determine the statistical significance of the factor responses, the response surface approach allows determining the statistical significance of each factor through the fitting of only 10 polynomial coefficients to 27 data points. Table 4 shows the factors values evaluated for the two slags, which were selected based on information reported in the literature.

The tests were performed in Erlenmeyer flasks and using synthetic solutions with initial concentrations of 6 mg/L As and 600 mg/L B; the slag doses ranged from 3 to 7 g/L, as specified by the experimental design. After preparing the suspensions without adjusting pH, all flasks were placed for mixing in an oscillating shaker at 250 rpm and using the temperature specified by the experimental design. After 6 h of mixing, 1 mL of each sample was filtered on 0.45 µm membranes (Millipore, cellulose esters). The experimental conditions were determined from kinetics and isotherms determined in earlier research, yielding equilibrium reaction data for As(V) as: $T_{eq} = 2.5$ h and $q_e = 1.99$ mg/g with Slag-2 and for B: $T_{eq} = 4$ h and $q_e = 1.75$ mg/g with Slag-1 (Mercado-Borrayo et al. 2014).

Table 4 Natural and corresponding scaled values (− 1, 0, 1) for removal of As(V) and B with slags

Factors	Levels		
	− 1	0	1
Temperature (°C)	25	35	45
Dose of slag (g/L)	3	5	7
pH (Slag-1)	7	9	11
pH (Slag-2)	6	8	10

Removal tests of arsenic and boron from geothermal wastewater

A geothermal wastewater sample was collected in the reinjection well of Los Humeros geothermal field to perform removal tests using the optimal values of the significant factors found by means of the response surface. The initial chemical composition of the wastewater is presented in Table 5 (González-Partida et al. 2005). The same experimental methodology described above was used in these experiments, in a two-step process, i.e., by first using Slag-1 for boron removal and then Slag-2 for arsenic(V) removal, both under the optimal conditions as determined using the synthetic solutions.

Solidification/stabilization of saturated slag

A solidification/stabilization treatment was used for both slags; 60% commercial cement was mixed with 40% saturated slag in a glass vessel at room temperature, adding water to prepare the mixture and then left to cure ate ambient conditions. As per Mexican norm NOM-052-SEMARNAT (2005), this product was evaluated by a certified laboratory. The norm includes tests for corrosivity, flammability, explosivity, reactivity and environmental toxicity, the latter being the only relevant question in this case.

Analytical techniques

The concentration of arsenic(V) was measured using the molybdenum blue spectrophotometric method (Rao and Rajan 1993), with ammonium molybdate (Fermont, 81.6%), hydrazine sulfate (Aldrich, 99%) and potassium bromide

Table 5 Average concentrations of ions characteristics of wastewater from four geothermal fields in Mexico

Geothermal fields	Li	Na	K	Mg	Ca	B	As^-	Cl	HCO_3	SO_4	SiO_2
Cerro Prieto	320	1.5×10^5	4×10^4	nr	1×10^4	500	30	3×10^5	nr	170	4×10^4
Tres Vírgenes	19	4297.5	737.5	0.85	274	157.5	5.39	7903	30.15	18.45	539
Los Azufres	23.82	4370.5	23.81	0.5	53.84	278.5	14.4	2705.8	11.63	43.14	776.75
Los Humeros	0.59	195.04	28.31	0.14	1.48	580	5.8	72.74	110	77.68	520.90

The concentrations of all compounds are expressed in mg/L

nr not reported

(Aldrich, 99%). The detection limit was 0.01 mg/L As, and the calibration curve showed a linear correlation coefficient $R = 0.997$. The concentration of boron was quantified using the spectrophotometric carmine method (Spielholtz et al. 1974). The detection limit of this method is 0.2 mg/L B and $R = 0.999$.

To explain the removal mechanism, slag grains were observed in a Philips XL20 Scanning Electron Microscope with standard Everhart–Thornley secondary electron detector and solid-state backscattered electron (BSE) detector. Observations were made on uncoated samples using atomic number contrast with BSE at an accelerating voltage of 20 kV. Energy dispersive X-ray spectroscopy was executed with a solid-state Oxford 7593 detector. Slag samples were observed before and after removal tests. "Blank" samples were produced by exposing the slags to distilled water under identical conditions as in the removal tests.

For SEM observations, 25 grains of slags in the size range of 20–50 µm were selected from randomly chosen observation fields, analyzing 3 or four grains per field, selected in the size range of 100 µm way and chosen such that the grains observed in a single field showed significant differences in morphology and/or composition. A fully random and statistically representative analysis is not feasible due to the large variation of particle sizes, morphology and composition; the present approach allowed to find sufficient grains in each condition (raw material, blank samples, samples after removal tests) to reach relevant conclusions.

Results and discussion

Statistical analysis of the removal data of arsenic and boron from the synthetic solution

The statistical models of As(V)-Slag-1, As(V)-Slag-2, B-Slag-1 and B-Slag-2 are shown in Eqs. 1–4 (nonsignificant terms are omitted).

As-Slag-1	$\%\ \text{Removal} = 46.74 - 0.99x + 3.29y + 1.07xy + 11.74z + 0.78yz$	Eq. 1
As-Slag-2	$\%\ \text{Removal} = 74.63 - 6.25x + 3.05x^2 + 2.54y + 18.75z + 3.59xz$	Eq. 2
B-Slag-1	$\%\ \text{Removal} = 98.90 - 3.06x - 5.75x^2 + 1.76y + 6.16z - 1.35xz - 5.09z^2$	Eq. 3
B-Slag-2	$\%\ \text{Removal} = 75.23 - 1.83x - 8.34x^2 + 1.60y + 8.49z + 1.10xz$	Eq. 4

where x: temperature, y: slag dose and z: pH (scaled values, see Table 4).

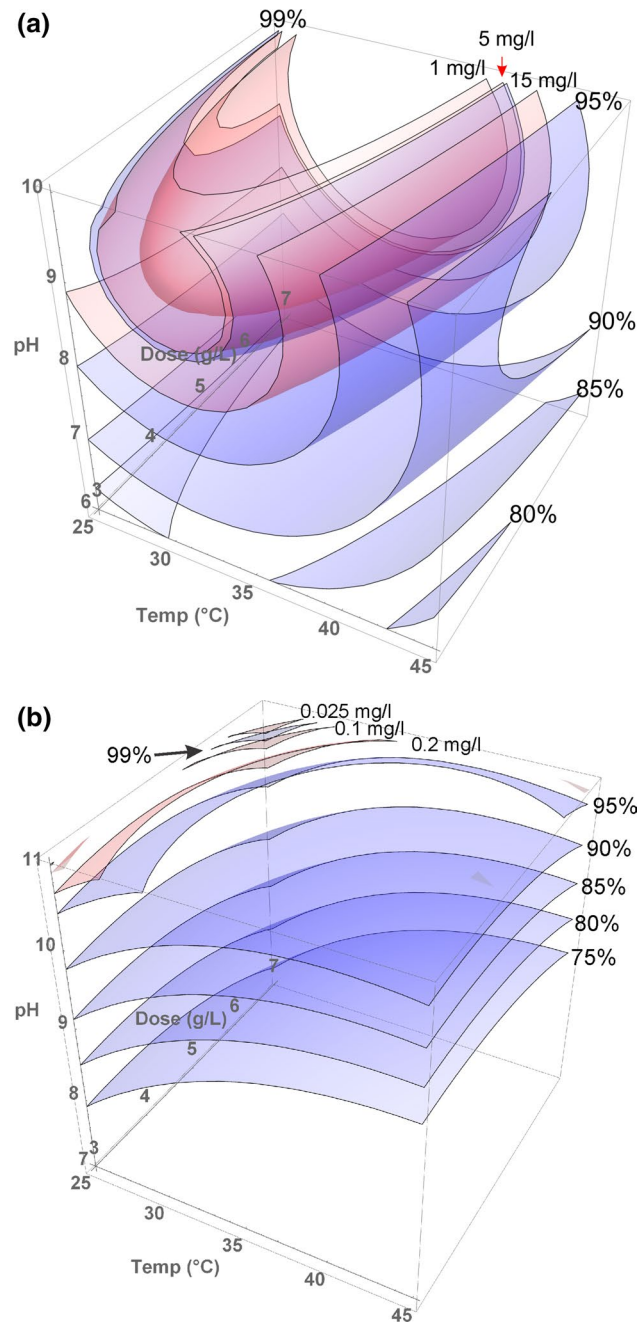

Fig. 1 Response surfaces of the B-removal using Slag-1 (**a**) and As(V) using Slag-2 (**b**). Surfaces of constant removal (%) are plotted as a function of temperature, pH and slag dose

Figure 1a, b shows the response surfaces of both slags as a function of the scaled values of the experimental factors. Only the results of the slags showing the best removal of pollutants are illustrated. Figure 1a is a graphical representation of Eq. 3 (B-removal with slag 1), Fig. 2b corresponds to Eq. 2 (As-removal with slag 2). Because the response surface is determined by the simultaneous variation of three parameters, surfaces of constant removal efficiency are

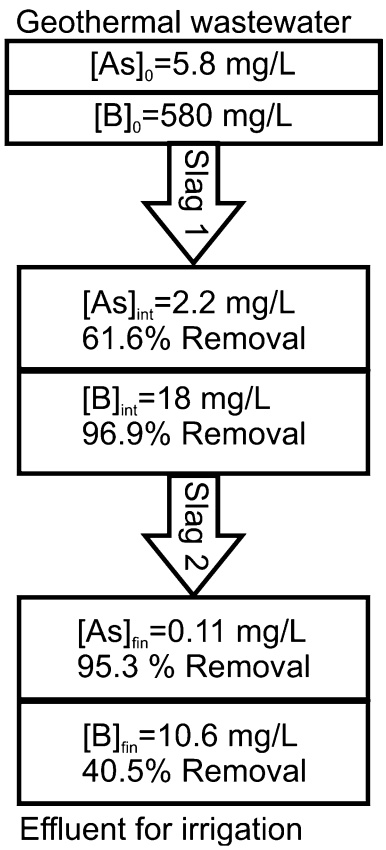

Fig. 2 Treatment train for the removal of As and B from geothermal wastewater using two different slags

presented. The blue contours show the removal efficiency (%), as obtained from experiments. The red contours correspond to constant levels of removal (in terms of residual concentration), with levels chosen according to environmental regulation.

B-removal ranged from 80 to > 99% using Slag-1 (blue surfaces in Fig. 1b). The concentrations of 1 mg/L B (tolerance for moderately sensitive crops), 5 mg/L B (tolerant crops) and 15 mg/L B (very tolerant crops) are illustrated in the graph by red surfaces. For the latter concentrations, the removal must be > 95%, which can be achieved easily under the experimental conditions tested here.

The As (V) removal ranged from 75 to 99% using Slag-2; when considering the limit concentration of this pollutant in wastewater treated for irrigation and an initial concentration of 6 mg/L As, a final content of 0.2 mg/L can be obtained with 96.6% of efficiency, and 0.1 mg/L As can be achieved with 98.3%. A contour is added which represents a residual concentration of 0.025 mg/L As, which would correspond to the Mexican standard for drinking water (*Modificación de la* NOM-127-SSA1 1994). It can be seen that even this level is within reach of the proposed process.

Table 6 Optimization of the removal of arsenic and boron for both slags in synthetic solution

Factor	Natural value	$(mg/L)_{fin}$	% Removal
Optimization of removal As-Slag-2			
x: Temperature (°C)	25	0.012 mg/L As	99.8
y: Dose of slag (g/L)	7		
z: pH	10		
Optimization of removal B-Slag-1			
x:Temperature (°C)	35	6 mg/L B	99.0
y: Dose of slag (g/L)	7		
z: pH	9		

Optimization of the removal process of arsenic and boron from synthetic solutions

Table 6 shows the unscaled values of the factors, the final concentrations and the removal of As(V) by Slag-1 and B by Slag-2, according to the experimental results for the synthetic solution. The effluent can be used for irrigation of tolerant crops (Table 1), since the final concentrations of boron (6 mg/L) and arsenic (0.012 mg/L) meet the criteria proposed for irrigation (0.1–2 mg/L As) for this type of crops.

Table 7 compares removal data of some materials described in the literature to the optimal results obtained in this work. The initial concentrations of pollutants in the present work are higher than the values reported in the literature, and lower doses of slags were employed in this research as compared to the amount of reagents used in Table 6, at a similar pH value.

Removal tests of arsenic and boron from a geothermal wastewater

As(V) and B were removed from a geothermal wastewater using the optimal conditions obtained in the experimental designs using the synthetic solution for both slags (Table 6). The treatment train using both slags is illustrated in Fig. 2, as well as the final concentration and the removal of pollutants

Table 7 As and B studies by adsorption process with non-conventional low-cost adsorbents

Adsorbent	$(mg/L)_o$	Doses (g/L)	PH	Time (h)	Temperature (°C)	%	References
Removal of arsenic with non-conventional low-cost adsorbents							
Slag 2: This work	6	7	10	6	25	99.8	
Metallurgical slags	1.40	nr	10	7	nr	80	Mohan and Pittman (2007)
Steel	10	20	7	nr	nr	85	Mohan and Pittman (2007)
Iron oxide-coated rock	nr	13	nr	nr	nr	99	Ilahi and Ali (2017)
Hematite/goethite	0.07–0.5	2	2–10	24	nr	80	Mamindy-Pajany et al. (2009)
Goethite	12	2.5	2.5	20	22	95	Asta et al. (2009)
Maghemite	0.25	5	3–9	5	23	95	Tuutijärvi et al. (2009)
Removal of boron with non-conventional low-cost adsorbents							
Slag 1: This work	600	7	9	6	35	99	
Red mud	12–200	1–8	2–7	4	nr	> 95	Cengeloglu et al. (2007)
Fly ash	600	1–5	2–11	8	25–45	90	Kashiwakura et al. (2009)
Carbon and fly ash	5	8–10	3–12	6	nr	> 90	Polat et al. (2004)

nr not reported

obtained in each removal stage. In the first step with Slag-1, the arsenic concentration decreased to 2.23 mg/L; in the second stage, the concentration was of 0.11 mg/L As(V) using Slag-2. This value is within the range (1 mg/L As) of international criteria proposed for agricultural irrigation water. The residual content of boron in the first removal step was 17.91 mg/L B; in the second one the effluent contained 10.65 mg/L, which meets the criteria recommended for very tolerant crops (6 mg/L B to 15 mg/L B) such as asparagus, sweet corn, cotton, sorghum and celery.

Solidification/stabilization of saturated slag

The solidification/stabilization process produced a solid with light gray color. According to the procedure defined in NOM-052-SEMARNAT (2005), the solid was classified as non-hazardous. Release of toxic substances was below the following values: Arsenic 5 mg/L, barium 100 mg/L, cadmium 1 mg/L, chromium 5.0 mg/L, mercury 0.2 mg/L, silver 5.0 mg/L, lead 5.0 mg/L and selenium 1.0 mg/L, as defined in the norm. From the removal mechanisms presented in the next section, it follows that the contaminants form stable precipitates on the slag surfaces. Regeneration of the slag for further use in the removal process is therefore not considered, but use in certain building applications is a logical option based on the results presented in this section.

Analysis of the removal mechanisms

The starting hypothesis of this work was that metallurgical slags would remove As (V) and B by means of adsorption. This hypothesis was based on the results of several authors (Kan et al. 2005; Fuente and Muñoz 2009; Chimenos et al. 2003) who have shown that these metalloids are removed by crystalline phases of certain metal oxides such as maghemite, portlandite, periclase and brucite, in accordance with the following reversible and irreversible adsorption reactions (Eqs. 5–10).

Reaction in metallic surface

$Me^{2+} + 2H_2O \leftrightarrow Me(OH)_2 + 2H^+$ Eq. 5 Hydrolysis

$Me^{2+} + 2OH \leftrightarrow Me(OH)_2^+$ Eq. 6 Hydroxylation

Boron

$B(OH)_3 + H_2O \leftrightarrow B(OH)_4^- + H^+$ Eq. 7 Dissociation of B

$Me(OH)_2^+ + B(OH)_4^- \leftrightarrow$ 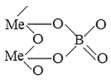 Eq. 8 Physisorption or chemisorption of B

Arsenic

$AsO(OH)_3 + H_2O \leftrightarrow H_2AsO_4^- + H_3O^+$

$H_2AsO_4^- + H_2O \leftrightarrow HAsO_4^{2-} + H_3O^+$

$HAsO_4^{2-} + H_2O \leftrightarrow AsO_4^{3-} + H_3O^+$ Eq. 9 Dissociation of As

$Me(OH)_2^+ + AsO_4^{3-} \leftrightarrow$ 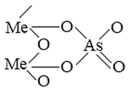 Eq. 10 Physisorption or chemisorption of As

where Me^{2+} is a metal ion.

However, the low surface area of the slag makes such adsorption hypothesis difficult to maintain. The calculated surface area for slag 1 was equal to 7.34 m^2/g, and for Slag-2 of 0.34 m^2/g. The BET-isotherm (Fig. 3) shows that no significant mesoporosity (2–50 nm) or microporosity (< 2 nm) is present. The problem is illustrated by a simple

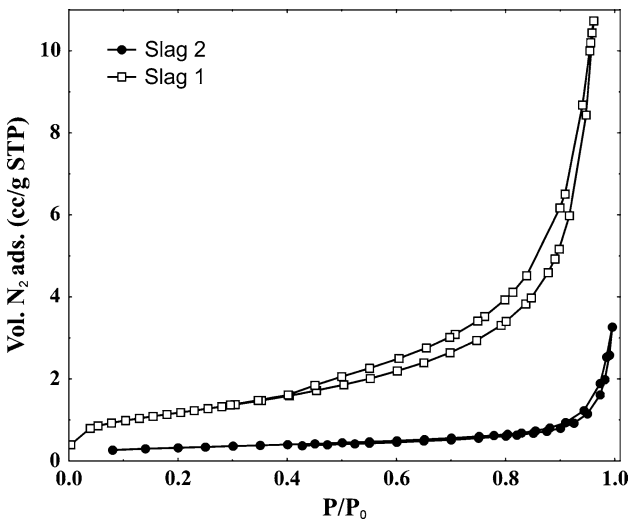

Fig. 3 Nitrogen adsorption isotherms for both slags

order-of-magnitude calculation. If one assumes that the entire available surface area is covered by a monolayer of densely packed spherical ions with radius equal to that of the borate-ion (191 pm) and $H_2AsO_3^-$ (840 pm), respectively, it is found that such monolayer cannot contain more than 7.3 mg of B adsorbed on 7 g of Slag-1 and 0.37 mg of As(V) on 7 g of Slag-2 under optimal operating conditions. This is 80 times less than the value obtained in practice for B on Slag-1 and 16 times less for As(V) on Slag-2. This excludes monolayer adsorption as a possible process. Even if a multilayer adsorption is considered to some extent, the amount of metalloids removed is too high; this means that adsorption is unlikely to be the principal removal mechanism.

SEM observations provide a first explanation on the alternative mechanisms involved. It was clear from the comparison of 25 grains each in the original material, blank samples and removal test samples that there were large differences between the three states. Representative examples of the SEM observations are presented in Fig. 4 (4A: slag 1, blank sample, 4B: slag 1, blank sample, 4C: Ca-rich grain in slag 1 (blank), 4D, similar as 4C, after exposure to B-containing solution, 4E: slag 2, blank. 4F: similar as 4E, after exposure to As-containing solution).

Figure 4a presents an example of a eutectic microstructure in the slag blank sample, which was revealed by the exposure to distilled water. Figure 4b presents a grain covered with Fe-based crystals in the blank sample, providing evidence of dynamic dissolution–precipitation. Structures like A and B were not seen in the raw material; structures like B were very rare even in the blank material. Figure 4c presents a Ca-rich grain of the steel slag with observable surface porosity, probably due to selective leaching during exposure to distilled water. Figure 4d shows a similar grain, but covered with Fe-rich deposits after exposure to the B-containing synthetic solution. Figure 4e presents a grain of iron slag, showing selective leaching in the form of pits (a) and grooves (b) of the Ca-rich phase in a binary eutectic with iron oxide. Figure 4f corresponds to a similar grain covered with iron-rich deposits, in the form of crusts (c) or as a very thin layer, which still allows observing the underlying eutectic lamellae (d).

From the comparison of the original with the blank samples, it followed that a leaching process was active because some grains show irregular surfaces in the blank due to selective dissolution, others show preferential dissolution of one of the phases in a two-phase microstructure, while still others reveal microstructures which were not visible in any of the original grains, indicating that these were covered by a product that was leached during the blank tests (Fig. 4) (see also Mombelli et al. 2016). In the presence of the metalloid anions, new deposits are formed which take the form of porous crusts in the case of Fig. 4b on Slag-1 and more continuous crusts for As(V) on Slag-2. In the latter case, some grains are covered with a thin layer of new deposits (Fig. 4f). The use of BSE allows detecting the underlying substrate, but it shall be reminded that the secondary electron penetration is a few µm under the present observation conditions (Goldstein et al. 2012), so what is seen in the image is not the result of a few adsorbed layers of atoms but a thin crust of iron-rich material covering the substrate.

These observations provide a strong indication that the removal mechanism is one of dissolution and co-precipitation, with the precipitates capturing the metalloids in their structure. There are three aspects of this process to be taken into account. Firstly, it has been indicated that species like calcite have a sufficiently high solubility to be in a dynamic state of dissolution/re-precipitation, favouring co-precipitation with appropriate metals. The fact that the pH of the solutions increases to 10 upon slag addition is a clear indication of the leaching of alkaline species. Those metals with an ionic radius similar to that of Ca (e.g., Cd^{2+}, Mn^{2+} and Fe^{2+}) can readily enter the calcite structure and form surface

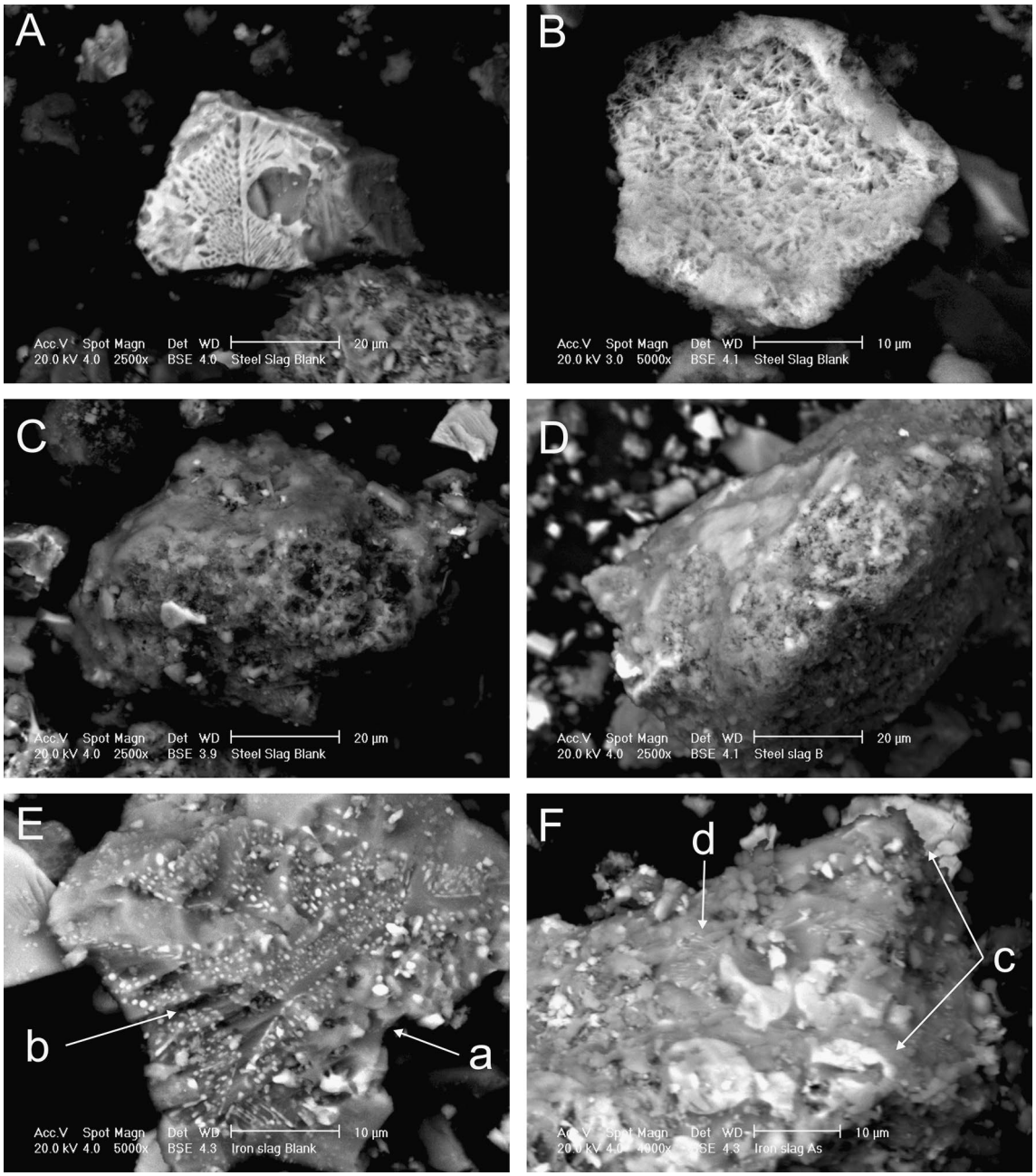

Fig. 4 SEM-observations of blank samples and samples after adsorption

co-precipitates (Zhou and Haynes 2010). The role of iron was described by Song et al. (2006) and by Li et al. (2010).

Secondly, it must be pointed out that in the case of slag, several components can be dissolved independently from their parent phases but will then interact with other species in solution. The presence of Fe-ions can then affect the solubility of Ca and Mg. The third aspect follows directly from the present observations. While precipitation is not entirely absent in the blank samples, its importance is limited as compared to the products used in the removal of As and B. This shows that the borate and arsenate ions play an active role in the promotion of precipitation. Bothe and

Brown (1999) investigated the role of calcium in such process, and Guan et al. (2009) described the complexation of calcium by iron. In the present work, as well as in the work of Song et al. (2006) and Li et al. (2010), the presence of As is below the detection limit of EDX, while B cannot be detected reliably in conventional EDX because of the use of a Be-window for the detector. Similarly, the relatively small amount of surface precipitates cannot be detected with precision by XRD. Techniques that are more sensitive will be used in future research to elucidate the precise reaction mechanisms and products formed in the processes reported here.

Conclusion

As an important progress with respect to earlier studies, this work demonstrates the feasibility of treating naturally contaminated geothermal wastewater with a two-step process, at the optimized conditions obtained for synthetic solutions of As(V) and B. This produced an effluent with an arsenic content (0.011 mg/L) which meets the criteria proposed by the US Environmental Protection Agency for irrigation. The final boron concentration (10.56 mg/L) was within the range proposed for very tolerant crops (6–15 mg/L). The performance of the two-step process is better than other processes using non-conventional reagents. The spent slag can be stabilized by conventional means (solidification/stabilization) and does not propose an environmental hazard.

It was found that removal of the metalloids involves the dissolution of iron, calcium and magnesium containing minerals in the slag and re-precipitation of insoluble products on the surface of the slag, which capture the pollutants in their structure. This observation presents a significant paradigm shift, because physisorption and chemisorption are more frequently considered as being responsible for the removal of metalloids by slags. A detailed analysis of the products and reactions involved is subject of ongoing research and may allow a more precisely directed process optimization strategy in future projects.

Acknowledgements B. Mercado-Borrayo thanks *Coordinación de Estudios de Posgrado*, UNAM for her PhD grant. M. Solís-López acknowledges support from *Dirección General de Asuntos del Personal Académico*, UNAM, for her postdoctoral grant. The project was supported by grants from the same organization under projects IV100616 and IT114511 as well as funds from Instituto de Ingeniería, UNAM.

References

Asta MP, Cama J, Martínez M, Giménez J (2009) Arsenic removal by goethite and jarosite in acidic conditions and its environmental implications. J Hazard Mater 171:956–972

Ayers RS, Westcot DW (1994) Water quality for agricultures. Food and Agriculture Organization, Rome

Bothe JJV, Brown PW (1999) The stabilities of calcium arsenates at 23° ± 1°C. J Hazard Mater B69:197–207

Cengeloglu Y, Tor A, Arslan G, Ersoz M, Gezgin S (2007) Removal of boron from aqueous solutions by using neutralized red mud. J Hazard Mater 21:415–422

Chillón AMF, Valero BL, Prats RD, Varó GP (2011) Approximate cost of the elimination of boron in desalinated water by reverse osmosis and ion exchange resins. Desalination 273:421–427

Chimenos JM, Fernández AI, Villalba G, Segarra M, Urruticoechea A, Artaza B, Espiell F (2003) Removal of ammonium and phosphates from wastewater resulting from the process of cochineal extraction using MgO-containing by-product. Water Res 37:1601–1607

Finster M, Clark C, Schroeder J, Martino L (2015) Geothermal produced fluids: characteristics, treatment technologies, and management options. Renew Sustain Energy Rev 50:952–966

Fuente GSM, Muñoz CE (2009) Boron removal by means of adsorption processes with magnesium oxide-modelization and mechanism. Desalination 249:626–634

Garg N, Singla P (2011) Arsenic toxicity in crop plants: physiological effects and tolerance mechanisms. Environ Chem Lett 9:303–321

Goldstein J, Newbury DE, Echlin P, Joy DC, Romig AD Jr, Lyman CE, Fiori C, Lifshin E (2012) Scanning electron microscopy and X-ray microanalysis: a text for biologists, materials scientists, and geologists. Springer, London

González-Partida E, Carrillo-Chávez A, Levresse G, Tello-Hinojosa E, Venegas-Salgado S, Ramírez-Silva G, Pal-Verma M, Tritlla J, Camprubi A (2005) Hydro-geochemical and isotopic fluid evolution of the Los Azufres geothermal field, Central México. Appl Geochem 20:23–39

Guan XH, Ma J, Dong HR, Jiang L (2009) Removal of arsenic from water: effect of calcium ions on As(III) removal in the KMnO4–Fe(II) process. Water Res 43:5119–5128

Güler E, Kaya C, Kabay N, Arda M (2015) Boron removal from seawater: state-of-the-art review. Desalination 356:85–93

Gupta VK, Suhas S (2009) Application of low-cost adsorbents for dye removal: a review. J Environ Manage 90:2313–2342

Hiriart G, Gutiérrez-Negrín LCA (2003) Main aspects of geothermal energy in Mexico. Geothermics 32:296–389

Ilahi SS, Ali CS (2017) Iron oxide and its modified forms as an adsorbent for arsenic removal: A comprehensive recent advancement. Process Saf Environ Prot 111:592–626

Kabay N, Köseoglu P, Yapici D, Yüksel Ü, Yüksel M (2013) Coupling ion exchange with ultrafiltration for boron removal from geothermal water-investigation of process parameters and recycle tests. Desalination 316:17–22

Kalel AN, Rahin MYA, Krishna LS, Abdul MZ, Salmiati S (2017) High concentration arsenic removal from aqueous solution using nano-iron enrich material (NIIEM) super adsorbent. Chem Eng J 317:343–355

Kan TA, Fu G, Tomson MB (2005) Adsorption and precipitation of an aminoalkylphosphonate onto calcite. J Colloid Interface Sci 281:275–284

Kashiwakura S, Kubo H, Kumagai Y, Hiroshi K, Kazuyo MY, Nakajima K, Nagasaka T (2009) Removal of boron from coal fly ash by washing with HCl solution. Fuel 88(7):1245–1250

Kourounis S, Tsivilis S, Tsakiridis PE, Papadimitriou GD, Tsibouki Z (2007) Properties and hydration of blended cements with steelmaking slag. Cem Concr Res 37:815–822

Lee JM, Kim JH, Chang YY, Chang YS (2009) Steel dust catalysis for Fenton-like of polychlorinated dibenzo-*p*-dioxins. J Hazard Mater 163:222–230

Li Y, Wang J, Luan Z, Liang Z (2010) Arsenic removal from aqueous solution using ferrous based red mud sludge. J Hazard Mater 177:131–137

Liu G, Dong X, Liu L, Wu L, Peng S, Jiang C (2014) Boron deficiency is correlated with changes in cell wall structure that lead to growth defects in the leaves of navel orange plants. Sci Hortic 176:54–62

Mamindy-Pajany Y, Hurel C, Marmier N, Roméo M (2009) Arsenic adsorption onto hematite and goethite. C R Chimie 12(876):881

Mercado-Borrayo BM, Schouwenaars R, González-Chávez JL, Ramírez-Zamora RM (2013) Multi-analytical assessment of iron and steel slag characteristics to estimate the removal of metalloids from contaminated water. J Environ Sci Health A Tox Hazard Subst Environ Eng 48:887–895

Mercado-Borrayo BM, Schouwenaars R, Litter MI, Montoya-Bautista CV, Ramírez Zamora RM (2014) Chapter 5: Metallurgical slags as an efficient and economical adsorbent of arsenic. Water reclamation and sustainability. Elsevier, New York

Mercado-Borrayo BM, González-Chávez JL, Ramírez-Zamora RM, Schouwenaars R (2018a) Valorization of metallurgical slag for the treatment of water pollution: an emerging technology for resource conservation and re-utilization. J Sustain Metall 4:50–67

Mercado-Borrayo BM, Contreras R, Sánchez A, Font X, Schouwenaars R, Ramírez-Zamora RM (2018b) Optimisation of the removal conditions for heavy metals from water: a comparison between steel furnace slag and CeO_2 nanoparticles. Arab J Chem. https://doi.org/10.1016/j.arabjc.2018.01.008

Modificación de la Norma Oficial Mexicana NOM-127-SSA1 (1994) Salud ambiental. Agua para uso y consumo humano. Límites permisibles de calidad y tratamientos a que debe someterse el agua para su potabilización. http://www.dof.gob.mx/nota_detalle.php?codigo=2063863&fecha=31/12/1969. Accessed 22 June 2018

Mohan D, Pittman CU (2007) Arsenic removal from water/wastewater using adsorbents: a critical review. J Hazard Mater 142:1–53

Mombelli D, Mapelli C, Barella S, Di Cecca C, Le Saout G, Garcia-Diaz E (2016) The effect of chemical composition on the leaching behaviour of electric arc furnace (EAF) carbon steel slag during a standard leaching test. J Environ Chem Eng 4:1050–1060

Moss SA, Nagpal NP (2003) Ambient water quality guidelines for boron. Ministry of Environment, Quebec

Newton AC (2016) Exploitation of diversity within crops: the key to disease tolerance? Front Plant Sci 7:665

Norma Oficial Mexicana NOM-052-SEMARNAT (2005) Que establece las características, el procedimiento de identificación, clasificación y los listados de los residuos peligrosos. México. http://dof.gob.mx/nota_detalle.php?codigo=4912592&fecha=23/06/2006. Accessed 22 June 2018

Oguz E (2005) Thermodynamic and kinetic investigations of PO_4^{3-} adsorption on blast furnace slag. J Colloid Interface Sci 281:62–67

Petousi I, Fountoulakis MS, Saru ML, Nikolaidis N, Fletcher L, Stentiford EI, Manios T (2015) Effects of reclaimed wastewater irrigation on olive (*Olea europaea* L.cv. 'Koroneiki') trees. Agric Water Manag 160:33–40

Piatak NM, Parsons MB, Seal R (2015) Characteristics and environmental aspects of slag: a review. Appl Geochem 57:236–266

Polat H, Vengosh A, Pankratov I, Polat M (2004) A new methodology for removal of boron from water by coal and fly ash. Desalination 164:173–188

Rao VSS, Rajan SC (1993) Spectrophotometric determination of arsenic by molybdenum blue method in zinc-lead concentrates and related smelter products after chloroform extraction of iodide complex. Talanta 40:653–656

Samatya S, Tuncel SA, Kabay N (2015) Boron removal from RO permeate of geothermal water by monodisperse poly(vinylbenzyl chloride-co-divinylbenzene) beads containing *N*-methyl-D-glucamine. Desalination 364:75–81

Smith SE, Christophersen HM, Pope S, Smith FA (2010) Arsenic uptake and toxicity in plants: integrating mycorrhizal influences. Plant Soil 327:1–21

Song S, López-Valdivieso A, Hernández-Campos DJ, Peng C, Monroy-Fernandez MG, Razo-Soto I (2006) Arsenic removal from high-arsenic water by enhanced coagulation with ferric ions and coarse calcite. Water Res 40:364–372

Spielholtz GI, Toralballa GC, Willsen JJ (1974) Determination of total boron in sea water by atomic absorption spectroscopy. Microchim Acta 62:649–652

Tomaszewska B, Bodezek M (2013) Desalination of geothermal wasters using a hybrid UF-RO process. Part I: boron removal in pilot-scale tests. Desalination 319:99–106

Tuutijärvi T, Lu J, Sillanpää M, Chen G (2009) As(V) adsorption on maghemite nanoparticles. J Hazard Mater 166:415–1420

Ungureanu G, Santos S, Boaventura R, Botelho C (2015) Arsenic and antimony in water and wastewater: Overview of removal techniques with special reference to latest advances in adsorption. J Environ Manage 151:3326–3342

US EPA (2012) Guidelines for water reuse. Washington, DC, 643 p. http://nepis.epa.gov/Adobe/PDF/P100FS7K.pdf. Accessed 22 June 2018

Wang B, Guo X, Bai P (2014) Removal technology of boron dissolved in aqueous solutions: a review. Coll Surf A 444:338–344

World Health Organization (2011) Guidelines for drinking-water quality, 4th edn. WHO Press, Geneva

Worldsteel Association (2014) Steel industry by-products. Fact Sheets, New York

Wu Q, You R, Clark M, Yu Y (2014) Pb(II) removal from aqueous solution by a low-cost adsorbent dry desulfurization slag. App Surf Sci 314:129–137

Zhou YF, Haynes RJ (2010) Sorption of heavy metals by inorganic and organic components of solid wastes: significance to use of wastes as low-cost adsorbents and immobilizing agents. Crit Rev Environ Sci Technol 40:909–977

View publication stats